Single Overload Effect in Short Crack

Tomoe Sudo[1, a], Masanobu Kubota[2, b] and Yoshiyuki Kondo[3, c]

[1]Graduate school of Kyushu University, 744 Motooka, Nishi-ku, Fukuoka, 819-0395, Japan

[2,3]Department of Mechanical Engineering, Kyushu University,
744 Motooka, Nishi-ku, Fukuoka, 819-0395, Japan

[a]te207363@s.kyushu-u.ac.jp, [b]kubota@mech.kyushu-u.ac.jp, [c]ykondo@mech.kyushu-u.ac.jp

Keywords: Fatigue, Single overload, Short crack, Crack closure, Retardation, Residual stress

Abstract. The effect of single overload on the retardation of fatigue crack propagation and crack arrest was examined on short crack less than a few hundred microns. The effect of stress ratio of baseline load was also investigated. The variation of crack closure stress caused by overload was measured. The retardation occurred even in short crack, which could be explained by the increase of crack closure stress caused by overload. The baseline stress ratio also affected the retardation. Retardation occurred even in 50 μm crack for baseline stress ratio R = 0. In the case of R = -1, however, no retardation occurred in short crack less than 100 μm since the increase of crack closure stress was restrained by the compressive stress of baseline load.

Introduction

The retardation of fatigue crack propagation caused by overload has been a major problem in fatigue crack research. Many researches have been done on this issue, mainly using a long crack [1]-[7]. The most typical understanding of this phenomenon is as follows. In the case of a long crack shown in Fig.1 (a), a large plastic zone is created ahead of the crack tip by overloading. The plastic deformation is constrained by the elastic body around the plastic zone, which introduces compressive stress field near of the crack tip. This compressive stress raises the crack closure stress [8] and hence the decrease of crack propagation rate or crack arrest occurs. In some case, the blunting of the crack tip may occur, which requires the re-initiation of crack and results in more retardation.

In the case of a long crack, strong enough constraint is given to the crack to cause compressive stress near the crack tip. However, the intensity of constraint around the crack is considered to be dependent on the crack size. In the case of a short crack, the plastic deformation and also the constraint is weaker than in a long crack. There should be a critical crack size which introduces an insufficient compressive stress field and hence causes no crack retardation.

In this study, the effect of overload on the increase of fatigue limit using short pre-cracked specimens was examined. The effect of stress ratio of the baseline load was also examined. Especially, the variation of crack closure stress introduced by overload was precisely investigated.

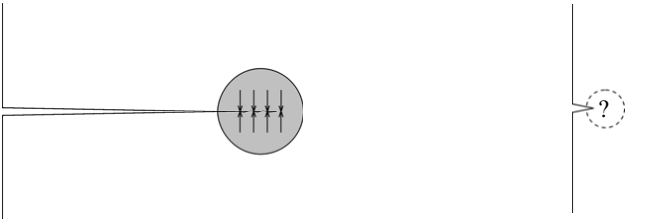

(a) Long crack (b) Short crack

Fig. 1 Residual stress at crack tip

Experimental Procedure

Material. The material used in this study was a low carbon steel designated as S25C by Japanese Industrial Standards. The chemical composition is shown in Table 1. The heat treatment of the material was normalizing. The mechanical properties after the stress relief annealing at 875 K are shown in Table 2. Figure 2 shows the microstructure of material after the stress relief annealing.

Table 1 Chemical compositions (mass %)

C	Si	Mn	P	S	Ni	Cr	Mo	Cu
0.27	0.17	0.46	0.016	0.018	0.03	0.12	-	0.03

Table 2 Mechanical properties after stress relief annealing

σ_y (MPa)	σ_B (MPa)	δ (%)	ϕ (%)
358	499	34.7	62.6

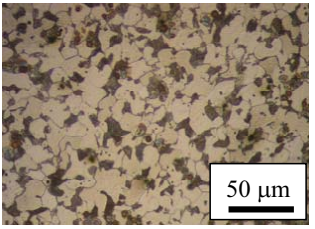

Fig. 2 Microstructure of S25C

Introduction of Short Fatigue Crack. Figure 3 shows the test specimen. A 100 μm deep notch shown in Fig. 3 (b) was machined through the thickness. A strain gauge was pasted directly on the notch to measure the crack opening displacement and another gauge was pasted to measure the bending moment applied to the specimen. The crack length was measured by the unloading elastic compliance method using these strain gauges [9].

At first, a short pre-crack was introduced at the notch root by fatigue. The conditions of fatigue pre-cracking were as follows; the stress amplitude was σ_a = 200 MPa and the stress ratio was R = -1.67. After the introduction of pre-crack, a part of the notch was removed by grinding until the depth of notch was equal to 20 μm. Three kinds of pre-cracked specimen whose crack depths including notch were 50, 100 and 170 μm. Figure 4 shows an example of 50 μm deep crack. As shown in the figure, the crack shape was two-dimensional. After that, the specimen was annealed at 875 K for 1 hour in vacuum to relieve the residual stresses introduced in the fabrication and pre-cracking processes.

Single Overloading Fatigue Test. Bending fatigue test was performed using the pre-cracked specimen. The stress in this paper was defined by the gross nominal bending stress at the crack location calculated based on the applied moment. Figure 5 shows the loading pattern. Small number of cyclic stress was applied prior to the overloading to measure the crack closure behavior before overload. The specimen with 50 μm deep crack was tested at R = 0 and -1, and specimens with 100 and 170 μm deep crack were tested at R = -1. Pulsating overload was applied whose maximum stress was 300, 350 and 400 MPa. Here, 400MPa was a fictitious elastic stress since it exceeded the yield strength of the material.

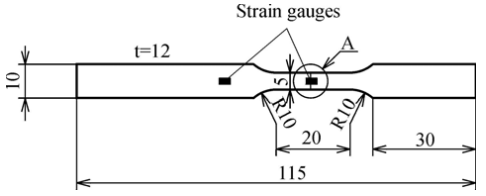

(a) Configuration

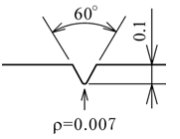

(b) Detail of A

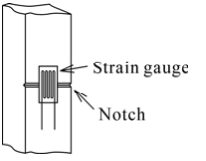

(c) Strain gauge for crack measurement

Fig. 3 Test specimen (Dimensions are in mm)

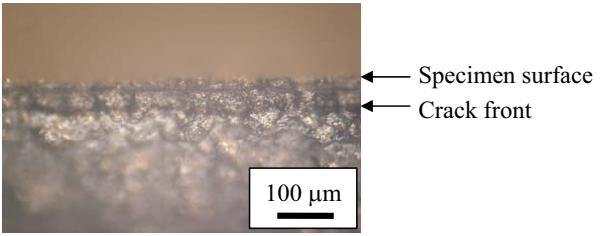

Fig. 4 Pre-crack

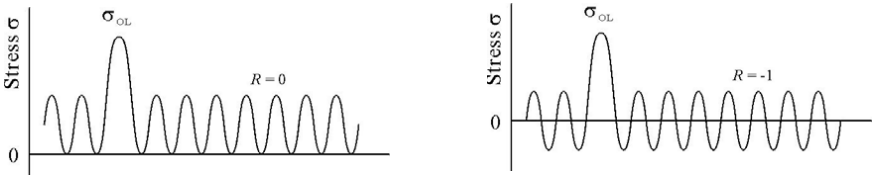

(a) $R = 0$ (b) $R = -1$

Fig. 5 Loading patterns

Test Results of Baseline stress Ratio $R = -1$

170 μm crack. Figure 6 shows the *S-N* curves for 170 μm deep crack tested at $R = -1$. No influence was seen in fatigue strength by the application of 300 MPa overload. The fatigue strength was increased when 350 MPa and 400 MPa overload were applied. Figure 7 shows the stress-offset displacement curves obtained at $\sigma_a = 140$ MPa. The crack opening stress in baseline test was almost zero during crack propagation. A similar trend was seen in the 300 MPa overloading test. In the case of 400 MPa overload test, however, the crack opening stress decreased just after the overload probably because of the blunting of crack tip. And then crack opening stress gradually increased as crack grew. Figure 8 shows the change of crack opening stress intensity factor with increase of crack length at $\sigma_a = 140$ MPa. The crack closure point after overload was raised much higher than the baseline data. This increase of crack opening stress after the application of overload should have caused the increase of fatigue strength. Figure 9 shows the fatigue crack propagation rate at $\sigma_a = 140$ MPa. The crack propagation rates in baseline test and 300 MPa overload test increased as the stress intensity factor increased.

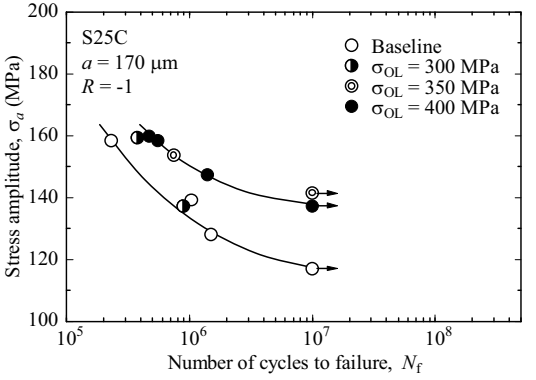

Fig. 6 *S-N* curves for 170 μm crack tested at $R = -1$

On the contrary, the crack propagation rate after 350 MPa and 400 MPa overload decreased and eventually the crack was arrested. Figure 10 shows the crack propagation rate shown against ΔK_{eff}. All data are in a narrow band. This indicates that the retardation of crack propagation was caused by the increase of crack closure stress by overload, which caused the increase of fatigue strength. This showed that a 170 μm crack was sufficient to introduce a compressive stress field ahead of the crack tip which raised the crack closure stress.

100 μm crack. Figure 11 shows the *S-N* curves for 100 μm deep crack tested at R = -1. No increase in fatigue strength was observed even by 400 MPa overload which caused a significant retardation in the case of 170 μm crack. Figure 12 shows the crack closure behavior. No overload effect is seen in the crack closure, which resulted in no influence of overload on fatigue strength.

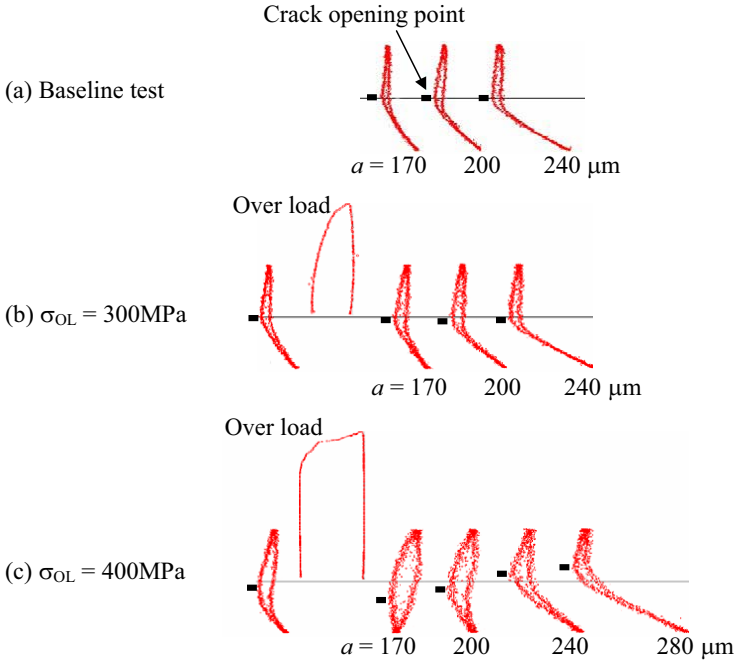

Fig. 7 Stress-offset displacement curves for baseline stress σ_a = 140 MPa

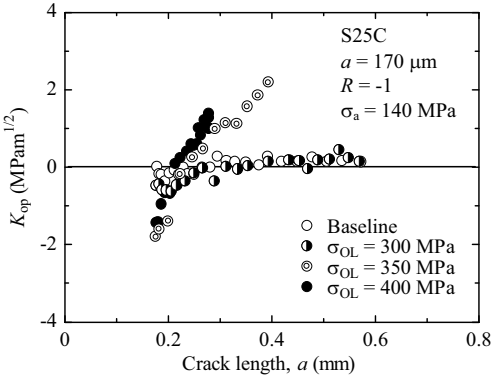

Fig. 8 Crack closure behavior at σ_a = 140 MPa

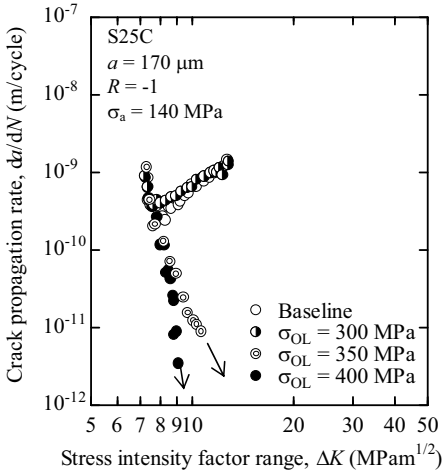

Fig. 9 Fatigue crack propagation rate at σ_a = 140 MPa

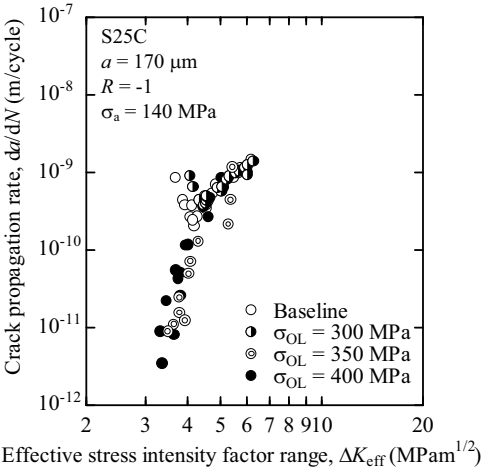

Fig. 10 Fatigue crack propagation rate shown against ΔK_{eff} at σ_a = 140 MPa

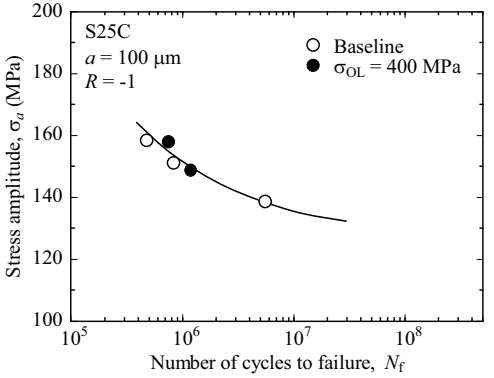

Fig. 11 *S-N* curves for 100 μm crack tested at R = -1

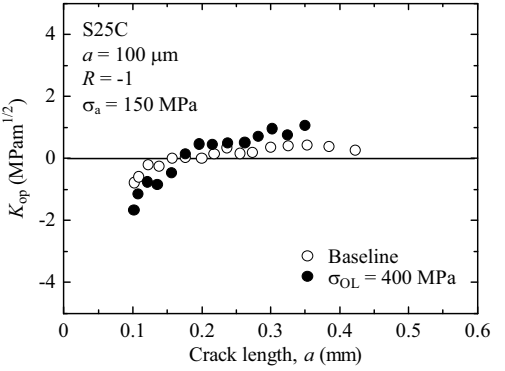

Fig. 12 Crack closure behavior at σ_a = 150 MPa

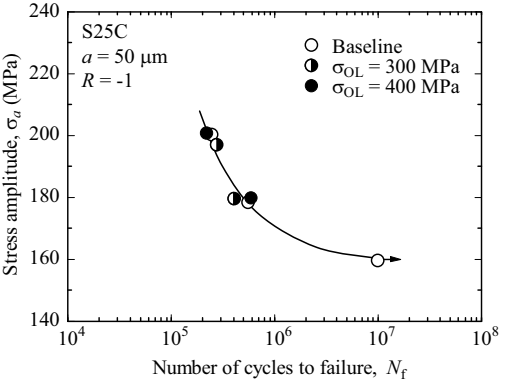

Fig. 13 *S-N* curves for 50 μm crack tested as R = -1

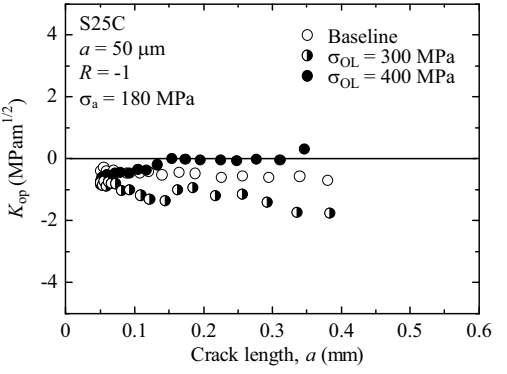

Fig. 14 Crack closure behavior at σ_a = 180 MPa

50 μm crack. Figure 13 shows the *S-N* curve for 50 μm deep crack tested at R = -1. The overload had no effect on the fatigue strength. Figure 14 shows the crack closure behavior. The crack opening stress was not raised at all even in overload tests. This is probably because the residual stress by overload was released by the compressive stress in the following fatigue loading. Hence no effect of overload on the fatigue strength was seen.

Since the nominal stress amplitude level becomes higher for shorter crack, the short crack experiences relatively high compressive stress in reversed loading. This prohibited the development of crack closure stress in short crack under reversed loading.

Test Results of Baseline stress Ratio R = 0

Figure 15 shows the *S-N* curves for 50 μm deep crack tested at R = 0. There was no effect of overload in the finite life region. However, the fatigue limit was increased in both overload stresses.

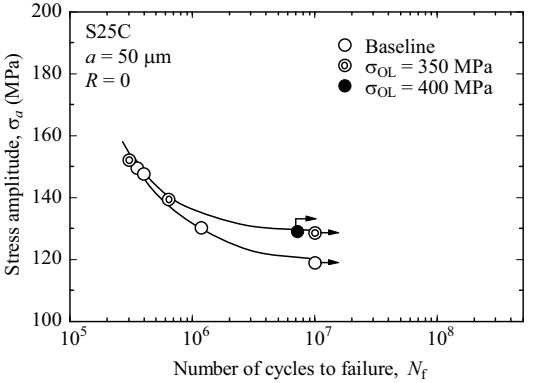

Fig. 15 *S-N* curves for 50 μm crack tested at R = 0

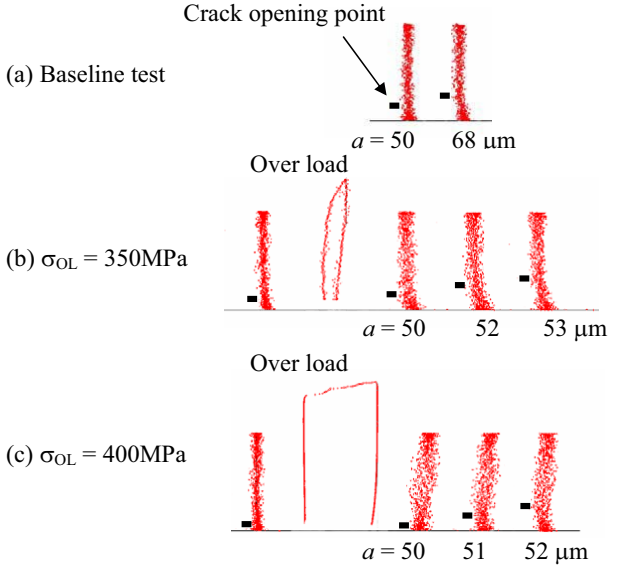

Fig. 16 Stress-offset displacement curves at baseline stress σ_a = 130 MPa

Figure 16 shows the stress-offset displacement curves at baseline stress σ_a = 130 MPa. Before the overload, the crack was almost closure free and the pre-crack was considered as an ideal crack. The crack opening stress increased immediately after the application of overload within an extension of crack by a few microns. It is quite different from the case of R = -1. The crack closure point was not raised by an overload in the case of a 50 μm deep crack at R = -1 as mentioned above. Figure 17 shows the relationship between crack opening stress intensity factor and crack length at σ_a = 130 MPa. The crack closure point was raised by the overload even in a 50 μm deep crack in the case of R = 0. It indicates that the crack length is not a unique factor that determines the occurrence of retardation but the baseline stress ratio is also concerned. This increase of crack closure stress after overload caused the increase of fatigue limit shown in Fig. 15. Figure 18 shows the fatigue crack propagation behavior obtained at σ_a = 130 MPa. The crack propagation rate of baseline test increased as the stress intensity factor increased. On the contrary, the crack propagation rate after overload decreased and then the crack was arrested. The crack propagation rate was evaluated using ΔK_{eff} as shown in Fig.19. In this case, the arresting behavior by overload is not so clearly shown because of scatter.

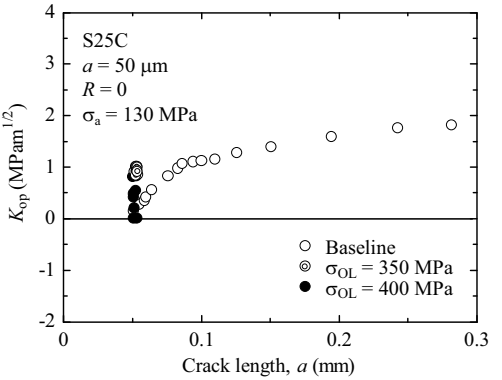

Fig. 17 Crack closure behavior at σ_a = 130 MPa

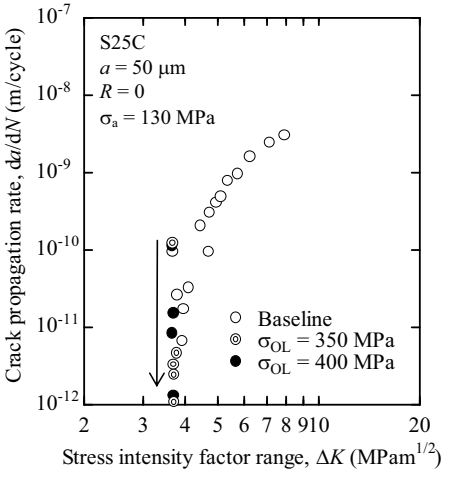

Fig. 18 Fatigue crack propagation rate at σ_a = 130 MPa

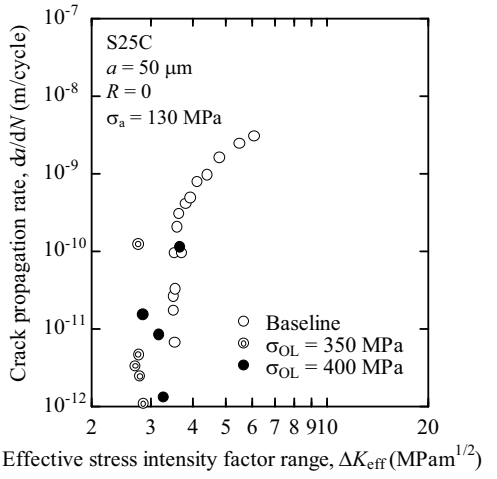

Fig. 19 Fatigue crack propagation rate shown against ΔK_{eff} at σ_a = 130 MPa

Summary

The effect of single overload on the retardation of crack propagation and crack arrest was examined using low carbon steel in the short crack regime. The obtained results are as follows.
(1) The retardation and crack arrest occurred even in short crack less than a few hundred microns.
(2) The cause of the retardation was the increase of crack closure stress introduced by an overload. The retardation behavior could be explained by the crack closure mechanism also in short crack regime.
(3) The crack length, which caused retardation, was dependent on the stress ratio of baseline load. The retardation occurred even in 50 μm crack at baseline stress ratio $R = 0$. However, the retardation was not apparent for crack less than 100 μm deep in the case of baseline stress ratio $R = -1$. This was because the increase of closure stress was restrained by the compressive stress in reversed loading.
(4) Table 3 shows the effect of overload in all test conditions. Relatively large overload stress approaching yield strength was needed to cause the retardation in short crack.

Table 3 Effect of overload in all test conditions

Baseline stress ratio $R = -1$

	Overload σ_{OL}		
Crack length	300 [MPa]	350 [MPa]	400 [MPa]
170 [mm]	× (2.50)	○ (2.92)	○ (3.33)
100 [mm]	× (2.14)	-	× (2.86)
50 [mm]	× (1.88)	-	× (2.50)

Baselien stress ratio $R = 0$

	Overload σ_{OL}		
Crack length	300 [MPa]	350 [MPa]	400 [MPa]
50 [mm]	-	○ (1.46)	○ (1.67)

- Not tested
× No effect of overloading
○ Increase of fatigue strength by overload
( ) $\sigma_{OL} / \sigma_{max\ baseline}$

Acknowledgement

The authors would like to express their thanks to Professor A.J.McEvily for helpful discussion.

References

[1] E.F.J.von Euw, R.W.Hertzberg, R.Roberts, *ASTM STP* 513, ASTM, West Conshohocken, PA, 1972, 230-259

[2] O.E.Wheeler, *Trans. ASME J. of Basic Engng.*, 1972, 94, 181-186

[3] G.J.Petrak and J.P.Gallagher, *Trans. ASME J. of Eng. Mat. Tech.*, 1975, 97, 206-213

[4] S.Matsuoka, K.Tanaka, M.Kawahara, *Engng. Fract. Mech.*, 1976, 8, 507-523

[5] R.J.Bernard, T.C.Lindley, C.E.Richards, *ASTM STP* 595, ASTM, West Conshohocken, PA, 1976, 78-97

[6] H.Bao, A.J.McEvily, *Met.Trans.*, 1995, 26A, 1725-2733

[7] C.Makabe, A.Purnowidodo, A.J.McEvily, *Int. J. of Fatigue*, 2004, 26, 1341-1348

[8] W.Elber, *ASTM STP* 486, ASTM, West Conshohocken, PA, 1971, 230-242

[9] Y.Kondo, C.Sakae, M.Kubota, M.Kashiwagi, *ASTM STP* 1461, 2005, 415-432